Spring 5-2019

Development and Analysis of a Methanol-to-Gasoline Reaction Setup for use in an Undergraduate Setting

Ryan Michael Beere

Development and Analysis of a Methanol-to-Gasoline Reaction Setup for use in an Undergraduate Setting

A Thesis

Submitted to the Faculty

Of

Rose-Hulman Institute of Technology

By

Ryan Michael Beere

In Partial Fulfillment of the Requirements for the Degree

Of

Master of Science in Chemical Engineering

May 2019

ROSE-HULMAN INSTITUTE OF TECHNOLOGY

Final Examination Report

Ryan M. Beere — Name

Chemical Engineering — Graduate Major

Thesis Title **Development and Analysis of a Methanol-to-Gasoline Setup for Use in an Undergradute Setting**

DATE OF EXAM: November 7, 2018

EXAMINATION COMMITTEE:

	Thesis Advisory Committee	Department
Thesis Advisor:	Gregory Neumann	CHE
	David Henthorn	CHE
	Stephanie Poland	CHEM

PASSED X **FAILED** _____

Abstract

Beere, Ryan Michael

M.S.Ch.E

Rose-Hulman Institute of Technology

May 2019

Development and Analysis of a Methanol-to-Gasoline Reaction Setup for use in an Undergraduate Setting

Thesis Advisor: Dr. Gregory Neumann

The primary goal of this research was to develop a framework for a setup for use in an undergraduate laboratory setting to study catalyzed reactions. A setup was developed with packed ZSM-5 catalyst for the Methanol-to-Gasoline (MTG) reaction. This research demonstrates and explains some of the trends that can be observed in catalytic reactions based on the effects of various process variables that can be used in a unit operations laboratory.

Process conditions such as temperature, particle diameter, and nitrogen flow rate were studied. The temperature trials confirmed that 375 $°C$ was the optimal temperature for methanol conversion. Selectivity towards higher molecular weight aromatics instead of the lower molecular weight aromatics was observed as temperature increased. Nitrogen flow rate was found to be inversely related to methanol conversion. No noticeable trends were found when the particle diameter was varied.

Keywords: Chemical Engineering, Heterogeneous Catalysis, ZSM-5, Methanol

Dedication

I'd like to dedicate this thesis to my parents who have both gone a long way in supporting me and helping me to get through school. Without them, I could not have made it this far.

Acknowledgements

I'd like to thank my advisor, Dr. Gregory Neumann, for his help and guidance in this project.

I'd like to thank all of my friends for helping me stay sane through everything and being there when I needed them.

I would also like to thank Mr. Frank Cunning and Mr. Lou Johnson for all of their help in using the equipment in the Rose-Hulman Chemical Engineering and Chemistry Departments.

Table of Contents

List of Figures

List of Tables

1. Introduction

World energy needs are constantly increasing, especially in developing areas. Energy needs are closely tied to economic increases such that if GDP doubles energy consumption increases by about 30% [1]. This is especially relevant in developing countries that need energy due to the energy costs associated with residential and industrial development. The energy needs of these areas have a large impact on the increasing needs of energy sources, such as liquid fuel. Due to this, liquid fuels will continue to be needed in increasing amounts in the foreseeable future [1]. Through the instruction of undergraduate engineering students, the relevancy of learning can be reinforced by current events. Giving context to specific tasks can aid students in the retention of the knowledge gained in the project.

A relevant liquid fuels reaction for the instructional purposes is the methanol to gasoline (MTG) reaction which can be used to teach students about an industrial process in this area. This allows students to follow the entire process from raw feed to consumer product which is rare in small scale unit operations experiments. Through use of this reaction, instruction can include some of the fundamental chemical engineering principles that are used in multiple industrial applications such as kinetics, mass transfer, and reusability. Catalytic reactors are common within the chemical industry and by way of this project, students will gain experience troubleshooting, analyzing, and controlling relatively simple reaction with multiple instructive objectives. The incorporation of products students use in their daily lives adds an element of motivation and empowerment. In addition to the importance of the production of liquid fuels, the reactor setup yields a wide variety of theoretical or empirical models that are encountered in chemical engineering courses and can be used with this experiment. The ability to tie together theoretical

concepts learned in the curriculum with a physical experiment has the potential to show how they work with an industrial application.

1.1. Liquid Fuels

Our current economy relies on fossil fuels as our primary source of liquid fuels. However, synthetic oil products are feasible. The production of these synthetic oils was proven via synthesis gas. There are two main paths for the conversion of synthesis gas, a mixture of carbon monoxide and hydrogen, to liquid fuels as shown in Figure 1-1. The most common path is the Fischer Tropsch (FT) reaction. This reaction is a catalyzed reaction that converts hydrogen and carbon monoxide into large hydrocarbons. This technology was used successfully by Germany during World War II and in South Africa during the Apartheid era. When this reaction is performed, refining is needed to get useable products such as naphtha and diesel from the large hydrocarbons that are not as useful as products [3].

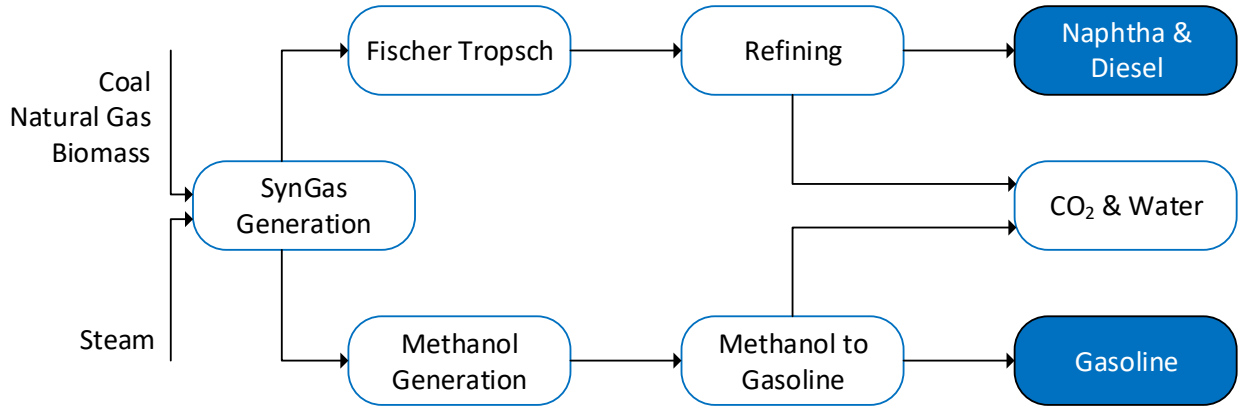

Figure 1-1. Conversion paths of carbon sources to liquid fuel adapted from [2].

Refining is a process which accepts crude oil as the feed and, through a series of separators and reactors, yields consumer products such as gasoline, diesel, heating oil, jet fuel, chemical feedstocks, waxes, lubricating oils, and asphalt. Refining is accomplished in three basic steps: separation, conversion, and treatment [4]. The separation step takes the crude oil and processes it in distillation units where products are separated into components called fractions by their boiling points. Heavy fractions, the gas oils, come out at the bottom and light fractions, like gasoline, come out at the top. Liquids such as kerosene come out in the middle. In the second step, conversion, some of the heavier fractions are converted into lighter more valuable products such as gasoline. The most common way to do this is by catalytic cracking. This process uses heat, pressure, and catalysts to crack large hydrocarbon molecules into smaller ones. In the final treatment step, some of the streams are combined from different units to create gasoline with proper octane levels and to meet other requirements such as vapor pressure and emission standards [4].

The Fischer-Tropsch synthesis route has been demonstrated as a viable way to utilize synthesis gas; however, due to the high energy consumption of the process and complex product mixtures; it has been suggested this cannot be the technology of the future [5]. An alternative method that has received considerable attention is the “Methanol Economy” [5]. In this analysis, the authors describe the ability to convert abundant natural gas sources directly to methanol which can take the place of traditional fuels such as gasoline, diesel, and natural gas. Although the suggestion that methanol can be used as an energy storage medium, it will be difficult to convert preexisting infrastructure over to solely a methanol economy. Therefore, the direct

conversion method to produce gasoline known as the methanol to gasoline process will be the focus of this thesis.

Like the Fischer-Tropsch synthesis, the MTG reaction is also catalyzed, but converts methanol to gasoline-range hydrocarbons, primarily in the $C_6 - C_{10}$ range. This process does not require a refining process like the Fischer Tropsch process because the products that are formed can already be used as gasoline [2]. The MTG process is a simple process which only requires methanol as feedstock and a conventional fixed bed reactor making it easily scalable as well as an excellent tool for instruction. There are many well-researched processes to generate methanol that make this method an attractive option for gasoline production from a variety of feedstock such as syngas, biomass, and water [7].

There are many sources of methanol that can be used for the MTG reaction. One of the most common ways to produce methanol is through the conversion of syngas to methanol as highlighted above. A traditional method for syngas production is from the steam reforming of methane, but other avenues including from incomplete combustion of coal have been used. Syngas is composed of carbon monoxide and hydrogen and can then be converted in a gas-phase reaction at high pressure in a fixed bed reactor directly to methanol [8]. Biomass can also be used to produce methanol. A process known as partial oxidation can convert the biomass into syngas which can be converted directly to methanol in a gas-phase reaction within a fixed-bed reactor as highlighted above. Electrical energy can also be used to convert water into hydrogen and oxygen [7]. The hydrogen can then be reacted with carbon dioxide to form methanol. There are a variety of methods for producing methanol suggesting that methanol can be an extremely abundant resource for use in the MTG reaction.

Recently, focus on methanol production has been on the development of catalysts that have a better yield of methanol. It has been found that copper-based catalysts are generally the best and most popular for methanol synthesis due to its higher activity. Zinc and aluminum-based catalysts have also been used for methanol synthesis [9].

Illustrated in Figure 1-2 is a simple example of an MTG process by ExxonMobil. In this example, methanol undergoes dehydration to form an equilibrium of dimethyl ether, methanol, and water. This mix is then sent to the reactors where the MTG reaction converts the mix to hydrocarbons in the gasoline range. This illustration contains three fixed bed reactors in parallel that can be cycled out when the catalyst becomes deactivated. Post reactors, the water is removed, and the gasoline is sent to recovery. This fixed bed process design is scalable up to 15,000 barrels of gasoline per day [2].

There are a variety of alternative fuel and energy sources with varying degrees of viability. While they all have their merits and uses, they are not yet close to being able to replace the needs for gasoline fully. These include some very high-level examples. Electric cars are becoming more popular but still are very cost prohibitive even though they have begun to be commercialized. Hydrogen fuel cell vehicles have been studied but still have many issues. One of the more significant issues is that hydrogen has a low energy content per volume compared to gasoline [10]. This means that hydrogen storage is a major issue in the commercialization of these types of vehicles. Some vehicles use Flex Fuel which is gasoline mixed with up to 85% ethanol. This still requires gasoline but is more renewable [11]. Despite the importance of investigating and studying alternative sources of energy, these alternative fuels are a long way away from

completely replacing gasoline. Therefore, studying the route of direct gasoline synthesis from methanol is relevant and appropriate for use in an undergraduate laboratory setting.

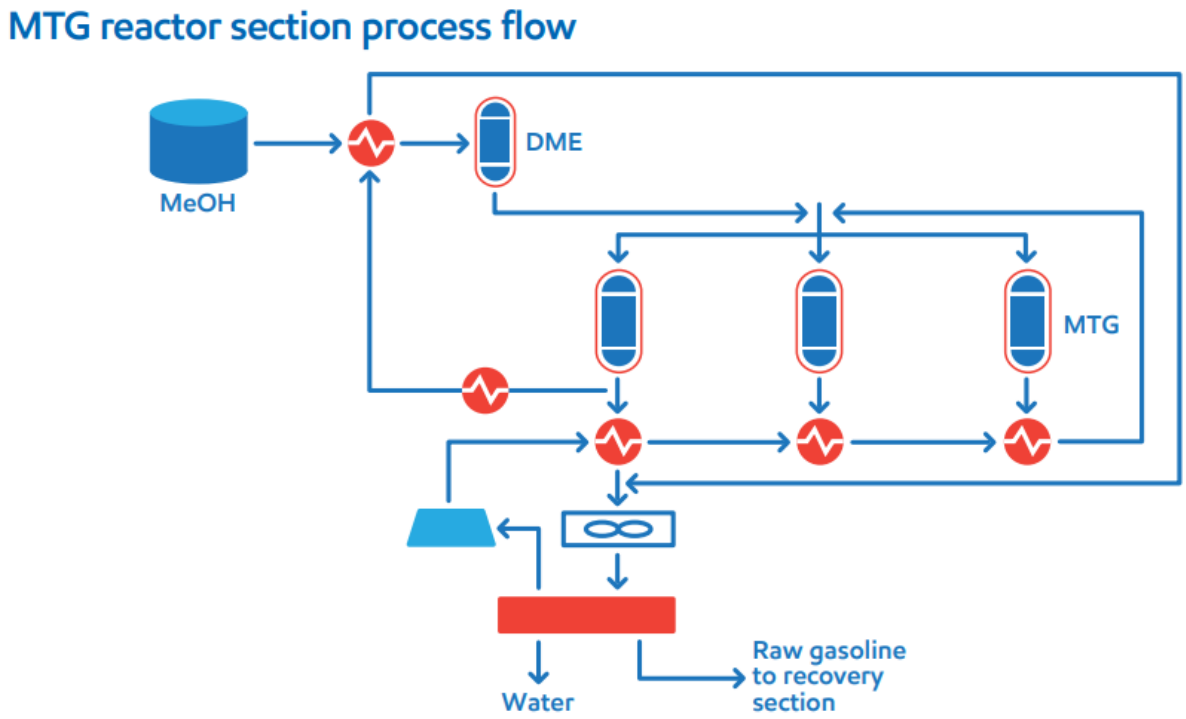

Figure 1-2. MTG process flow diagram from ExxonMobil [2].

1.2. Catalysts

Catalysts are commonplace in the chemical engineering industry and are thus valuable assets in the laboratory as a teaching tool. Many reactions require a catalyst to allow the reaction to proceed at reasonable process conditions and can, therefore, be used to teach many topics related to chemical reactions. Additionally, catalysts are normally reusable and are thus valuable as a learning resource because the initial investment can be offset by the fact that the catalyst can be used for multiple terms.

Catalysts are traditionally defined as a class of material that increases the rate of a chemical reaction. They do this by lowering the activation energy required for the reaction to occur as shown in Figure 1-3 [14]. From the dawn of civilization, catalysts have been used, but the field was not formally introduced until 1835 by Jöns Jacob Berzelius. By the nineteenth century, it was becoming clear, through experimentation, that most chemical processes benefited financially from the use of catalyst and it was said by Wilhelm Ostwald that "there is probably no chemical reaction which cannot be influenced catalytically" [15].

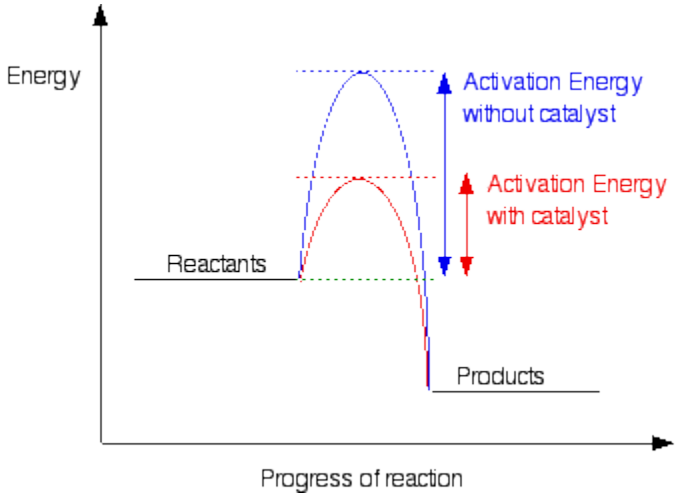

Figure 1-3. Activation energy with and without a catalyst [14].

When classifying catalysts, in general, they are separated into two categories: homogeneous and heterogeneous catalysis. A chemical reaction that is aided by a catalyst that is the same phase, typically liquid or gas, as the reaction medium is considered homogenous catalysis. On the other hand, heterogeneous catalysts are a different phase than the reactants. Typically, heterogeneous catalysis uses a solid catalyst that has either liquid or gaseous reactants flowing over it. During heterogeneous catalysis, reactants adsorb onto active sites on the surface of the catalyst. These active sites are where the reaction takes place. The product then desorbs

from the catalyst [16]. For the reaction studied in this paper, we use Zeolite Socony Mobil-5 (ZSM-5) as a heterogeneous catalyst. An advantage of using a heterogeneous catalyst is that it can be recovered and separated from the reactants/products without expensive separation techniques. An additional benefit is that if the catalyst becomes deactivated, it can be easily removed and regenerated for repeated use.

The most common reactor setup for heterogeneous catalysis is a fixed bed reactor. A fixed bed reactor contains the packed catalyst in a tube or pipe and is normally used with gas phase reactants that flow over the catalyst. Catalytic fixed bed reactors are used in many different industrial processes for various types of reactions [17]. In large scale processes, multiple fixed bed reactors can be used in parallel. This allows the deactivated catalyst to be changed out as the reactor is taken offline.

The first observation of hydrocarbon formation from methanol is credited to Mattox in 1962. Olefins in the $C_2 - C_5$ range were formed during methanol dehydration over NaX zeolite [18]. Similar results were found by others over a variety of catalysts. In 1974, Pearson was able to obtain larger yields of hydrocarbons including some aromatics with methanol dehydration over P_2O_5 at higher temperatures [18]. In 1976, Mobil discovered a shape-selective catalyst that allowed for conversion of methanol to gasoline with ZSM-5 [18].

The catalyst used in the MTG reaction is a ZSM-5 catalyst which has the repeating formula of $|Na_n^+(H_2O)_{16}|[Al_nSi_{96-n}O_{192}]$ where n is less than 27 [19]. ZSM-5 is an acidic catalyst and thus can be continuously used in acid catalyzed reactions and is primarily utilized by the petroleum industry for cracking large hydrocarbons. ZSM-5 is an aluminosilicate material giving

it highly acidic properties. Aluminum ions (Al^{3+}) replace silicon ions (Si^{4+}) in the lattice framework resulting in a proton (H^{+}) being needed to keep the material charge neutral. As a result, the Brønsted acidity of the catalyst is directly proportional to aluminum content [20].

In addition to the properties ZSM-5 has as an aluminosilicate material, it also has properties related to its physical structure. ZSM-5 is a zeolite that is defined by 10-membered rings as shown in Figure 1-4, and the channel size of these rings dictates the size of compounds that can traverse through the catalyst. The channel dimensions of the catalyst are approximately 5.4 X 5.6 Å, which limits larger compounds sterically. However, compounds in the gasoline range are able to diffuse in the catalyst during this reaction. The 10-membered rings are defined by a basic 12 atom building blocks as seen in Figure 1-5a that come together to form the chains in Figure 1-5b [21].

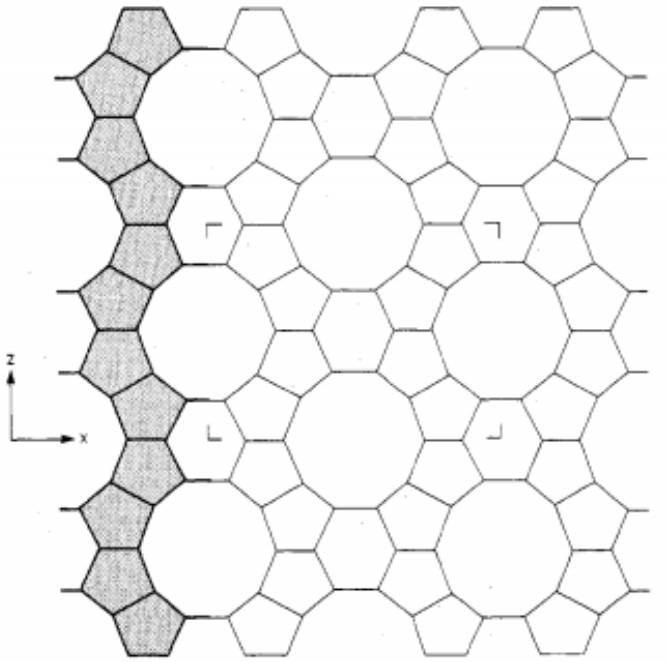

Figure 1-4. Diagram of ZSM-5 layer showing the 10-membered rings [21].

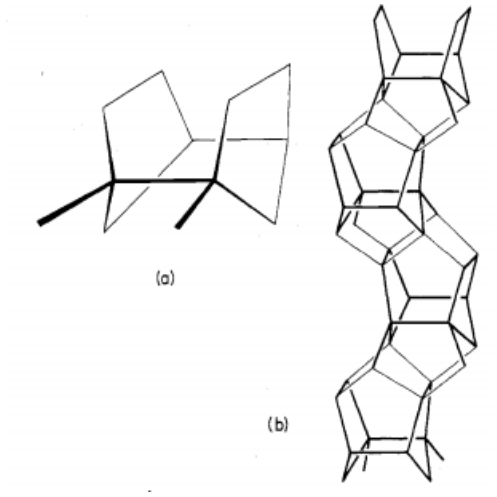

Figure 1-5. (a). 12-atom building block (b). Chain formed from building blocks [21].

In addition to speeding up the rate of reaction at a given temperature, catalysts can also sometimes take on a secondary role. They can help to control the slate of products in certain reactions. In the MTG reaction, ZSM-5 does this because the channel size and shape limit certain larger compounds, C_{11} aromatics and larger, from moving through the catalyst [21].

The primary goal of this research is to develop a framework for a setup that could be used with this reaction to study catalyzed reactions in an undergraduate laboratory setting. Because the Unit Operations Laboratory at Rose-Hulman Institute of Technology does not currently have a catalytic reactor available for undergraduate experimentation, there is a unique opportunity to introduce this project. There is a strong need to instruct students with industrially relevant equipment and projects. The introduction of heterogeneous catalysis will give students an opportunity to experimental with fundamental concepts such as kinetics, heat transfer, mass transfer all which learning how catalysts behave during operation. This will prepare them for experiences outside of academia.

1.3. MTG Mechanism

The MTG reaction is initiated by the formation of a "hydrocarbon pool" in the catalyst. The "hydrocarbon pool" consists of compounds that form inside the catalyst channels such as cyclic carbenium ions. These compounds undergo methylation and olefin elimination and act as reaction centers to form the desired products. Without this "hydrocarbon pool," the MTG reaction will not occur. It is believed that impurities in the methanol feed, the carrier gas, and incomplete combustion on the catalyst leave enough organics in order to form the pool. The required formation of these pools means that there is an observed kinetic induction period during which the reaction proceeds very slowly or not all [22].

In addition to a "hydrocarbon pool," methanol also has to undergo a dehydration reaction to form an equilibrium of methanol, dimethyl ether, and water. The methanol and dimethyl ether react with the reaction centers of the pool to form light olefins, like ethylene and propylene. Paraffins, aromatics, and heavier olefins are then formed. These reaction steps result in a product slate ranging from ethylene to polymethylbenzenes. As the reaction progresses and bigger compounds form, their mobility through the catalyst channels decreases with increasing diameter. Once the compounds get to the size of pentamethylbenzene, they start to become incapable of moving through the catalyst. This leads to deactivation and coking on the catalyst as the molecules fill up the active sites [23].

The pore size of the catalyst also plays a role in the shape selectivity of certain compounds of similar or equal molecular weights. For instance, para-xylene and ortho-xylene are both the exact same molecular weight, but the structure of p-xylene allows it to traverse through the

catalyst channels easier than o-xylene. Looking down the axis of the methyl groups on p-xylene shows that it has a smaller effective diameter when traversing through the channel than o-xylene. This type of shape selectivity occurs for all aromatics in the $C_8 - C_{10}$ range [21].

Catalyzed reactions are a significant part of many chemical engineering industries, such as the petroleum, pharmaceutical, and specialty chemical industries. Another goal in this research is to show and explain some of the trends that can be observed in catalytic reactions based on the effects of various process variables. Additionally, after the initial setup has been developed, possible improvements that could be made if more resources were available should be recommended.

2. Theory

In a fixed catalyst bed, there are multiple terms that need to be defined and calculated in order to fully define and analyze the reaction. In a packed bed reactor, the reactions occur on the surface of the catalyst. Therefore, instead of normalizing on the reactor volume, the catalyst mass is used for the reaction rate. This is shown in Equation 1 where W is catalyst weight [24].

$$-r_A' = \frac{mol\ of\ 'A' reacted}{time * W} \tag{1}$$

Conducting a mole balance over the differential catalyst bed yields Equation 2 [24].

$$\frac{dF_A}{dW} = r_A' \tag{2}$$

Substituting the definitions of fractional conversion into Equation 2, yields Equation 3 [24].

$$F_{A0}\left(\frac{dX}{dW}\right) = -r_A' \tag{3}$$

One important term when analyzing a fixed catalyst bed is weighted hourly space velocity (WHSV), defined as the weight of feed flowing through the reactor per unit weight of the catalyst per hour. In a fixed bed, the weight of the catalyst in the reactor is a constant (coking does not affect catalyst weight as it is not part of the catalyst); therefore, the only variable that changes and affects WHSV is the flow rate of feed. In this study, both methanol and nitrogen are flowing into the reactor. Methanol is the feed, and nitrogen is simply a carrier gas, so the nitrogen flow rate has no impact on WHSV. WHSV can be defined using Equation 4 [24]:

$$WHSV = \frac{F_A}{W} \tag{4}$$

In a fixed bed, flow across the bed creates a pressure drop, which is extremely relevant when conducting the analysis of the experiments. For an ideal gas, the concentration of a species is defined in Equation 5 where $\Theta_i = \frac{F_{i0}}{F_{A0}}$ [24].

$$C_i = C_{A0}\left(\frac{\Theta_i + v_i X}{1 + y_{A0}\delta X}\right)\frac{P}{P_0}\frac{T_0}{T} \tag{5}$$

For gas phase reactions Equation 5 yields Equation 6 [24].

$$C_A = \frac{C_{A0}(1 - X)}{1 + y_{A0}\delta X}\frac{P}{P_0}\frac{T_0}{T} \tag{6}$$

An example rate law is shown in Equation 7 [24].

$$-r_A' = kC_A^n \tag{7}$$

The rate law can then be written as Equation 8 when Equation 6 is substituted into Equation 7 [24].

$$-r_A' = k\left(\frac{C_{A0}(1 - X)}{1 + y_{A0}\delta X}\frac{P}{P_0}\frac{T_0}{T}\right)^n \tag{8}$$

From Equation 8, one can see that the larger the pressure drop across a bed, the smaller the reaction rate will be as this reduces $\frac{P}{P_0}$ [24].

In order to model the pressure drop across a bed, the Ergun equation as shown in Equation 9 can be used [24]:

$$\frac{\Delta P}{L} = \frac{150 * \mu * (1 - \epsilon)^2 * v_0}{\epsilon^3 d_p^2} + \frac{1.75 * (1 - \epsilon) * \rho * v_0^2}{\epsilon^3 * d_p} \tag{9}$$

where ΔP is the pressure drop across the bed, L is the length of the bed, μ is the viscosity of the fluid, ϵ is the void space in the bed, v_0 is the superficial fluid velocity, d_p is the particle diameter, and ρ is the density of the fluid. Equation 3 shows a few important things that are relevant to our experiment. As particle size increases, the pressure drop across the bed decreases. Additionally, as fluid velocity increases, the pressure drop across the bed increases. These two statements are important in determining the conditions with which we were able to run experiments [24].

In order for a reaction to happen, diffusion of the reactant from the bulk to the surface must occur. This rate of diffusion is defined in Equations 10 and 11 [24]. In these equations, k_c is the mass transfer coefficient. It is a function of particle diameter and fluid velocity [24].

$$rate = k_c(C_{Ab} - C_{As}) \tag{10}$$

$$k_C = \frac{D_{AB}}{boundary\ layer\ thickness} \tag{11}$$

The boundary layer thickness is defined as the distance between the solid and the point where the concentration of reactant is 99% of the bulk [24]. At low velocities, the boundary layer is thicker, and it takes longer for A to get to the surface. At high velocities, the boundary layer becomes very thin and offers little resistance to mass transfer. Particle size has the reverse effect [24]. As fluid velocity increases or particle size decreases, k_c increases until it reaches a plateau where $C_{Ab} \approx C_{As}$.As a result of this, the velocity of the fluid influences the rate of the reaction. Depending on the velocity at which the fluid flows, the reaction rate can end up in one of two regimes, diffusion-limited and reaction-limited. The diffusion limited regime occurs when the flow rate is slow enough that reaction happens faster than the external diffusion of the reactant into the catalyst [24]. Therefore, the reaction entering the catalyst is the step that limits the

reaction rate. The effect is shown in Figure 2-1. At these flow rates, the gas flow rate is fast enough that the rate exists in the reaction limited regime. As the flow rate increases the residence time decreases and the conversion goes down even though the rate stays the same [24].

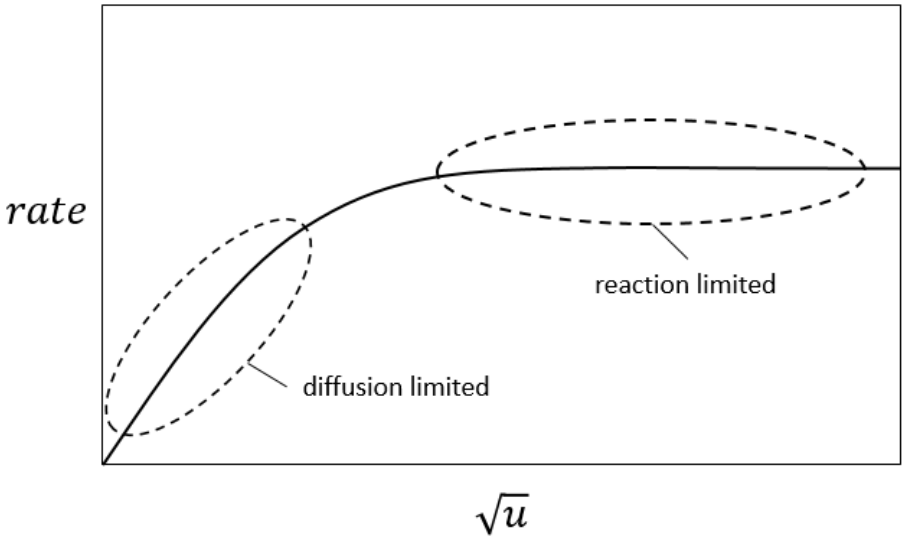

Figure 2-1. Velocity effects on reaction rate. Diffusion limited and reaction limited regimes [24].

A similar concept also can be applied to catalyst size. If the catalyst size gets too big, diffusion can only carry product from near the surface. To reach the inner surface of the catalyst it must diffuse from the surface through the pores of the catalyst pellets. The diffusivity in the catalyst is defined with Equation 12 where τ is tortuosity, ϕ_p is pellet porosity, and σ_C is constriction factor [24].

$$D_C = \frac{D_{AB}\phi_p\sigma_C}{\tau} \tag{12}$$

With the introduction of some dimensionless variables in Equations 13 and 14, we can develop the Thiele modulus. For these equations, it is assumed that C_{As} is the concentration of A at the surface of the catalyst and that the catalyst is spherical with radius, R [24].

$$\Psi = \frac{C_A}{C_{As}} \tag{13}$$

$$\lambda = \frac{r}{R} \tag{14}$$

Applying boundary conditions and using the molar differential equation we get Equation 15. The boundary conditions used are $C_A = C_{As}$ at $r = R$, and C_A is finite at $r = 0$ [24].

$$W_{Az} = -D_C \frac{dC_A}{dr} \tag{15}$$

Using chain rule and differentiating equations 13 and 14, we can get Equation 16 [24].

$$\frac{dC_A}{dr} = \frac{d\Psi}{d\lambda}\frac{C_{As}}{R} \tag{16}$$

Differentiating and substituting, we can finally get to Equation 17 [24].

$$\frac{d^2\Psi}{d\lambda^2} + \frac{2}{\lambda}\left(\frac{d\Psi}{d\lambda}\right) - \Phi_n^2\Psi^2 = 0 \tag{17}$$

Where

$$\boldsymbol{\Phi}_n^2 = \frac{k_n R^2 C_{As}^{n-1}}{D_C} \tag{18}$$

The Thiele modulus in Equation 17 and 18 is equal to Φ_n and is equal to the surface reaction rate over the diffusion rate. As the Thiele modulus gets bigger, the reaction rate goes down due to

internal diffusion limiting the reaction [24]. This is shown in Figure 2-2, where in this log-log plot the vertical axis is the effectiveness factor. The effectiveness factor relates the actual rate to the rate if the reaction were to take place only on the surface of the catalyst. If the reaction is unhindered by diffusion, this factor will be close to one. Because the Thiele Modulus has a strong dependence on the size of the catalyst particle, the larger the particle the greater the resistance to mass transfer and therefore less effective catalyst when analyzing the actual rate of reaction.

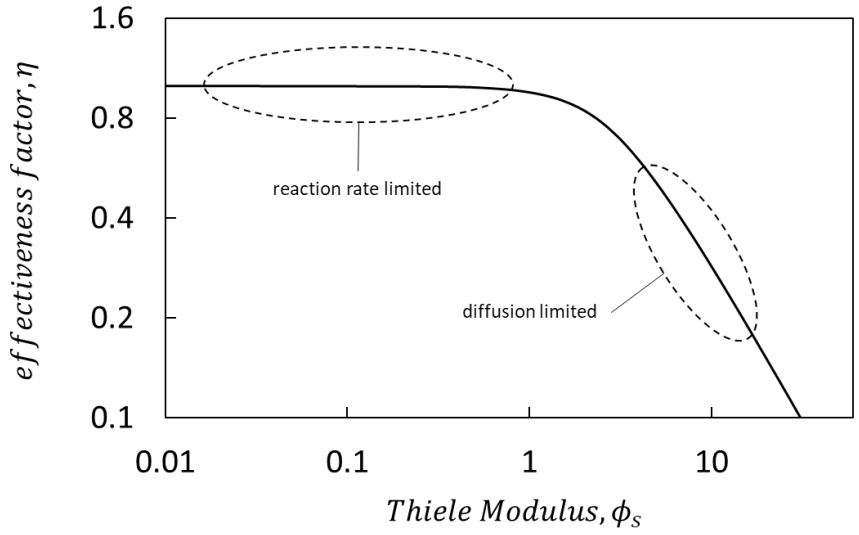

Figure 2-2. Diffusion limited and reaction limited regimes for internal diffusion through a spherical catalyst [24].

Considering these governing equations for a packed bed reactor, the MTG process can be used in the undergraduate laboratory setting to introduce these concepts discussed in this section as a hands-on project. The versatility of the project objectives as well as how these governing equations can be used in the laboratory will be discussed in Section 5, Educational Uses.

Table 2-1. Table of Variables for Theory Section

Variable	Definition	Variable	Definition
$r_A{}'$	Rate of A reacted per mass of catalyst	μ	Viscosity of the fluid
W	Mass of catalyst	ϵ	Void space in the bed
F_A	Flow rate of A	v_0	Superficial fluid velocity
F_{A0}	Flow rate of species A at the entrance	d_p	Particle diameter
X	Conversion	ρ	Density of the fluid
θ_i	$\frac{F_{i0}}{F_{A0}}$	k_c	Mass transfer coefficient
F_{i0}	Flow rate of species I at the entrance	C_{Ab}	Concentration of A at the boundary layer
C_i	Concentration of species I	C_{As}	Concentration of A at the surface of the catalyst
C_{A0}	Concentration of species A at the entrance	D_{AB}	Diffusion coefficient
v_i	Stoichiometric coefficient	D_c	Effective diffusivity
y_{A0}	Mole fraction of species A	ϕ_p	Pellet porosity
δ	Change in total number of moles over the moles of limiting reactant	σ_c	Constriction factor
P	Pressure	τ	Actual distance molecule travels over shortest distance between those two points
P_0	Pressure at the entrance	Ψ	Dimensionless concentration
T_0	Temperature at the entrance	λ	Dimensionless length
T	Temperature	r	Distance from center of catalyst
C_A	Concentration of species A	R	Radius of spherical catalyst
k	Rate constant	W_{Az}	Molar flux of species A
n	Rate order	Φ_n	Thiele Modulus
L	Length of bed		

3. Materials, Experimental Setup, and Procedures

A similar experimental setup and procedure were followed for all MTG reaction trials and was adjusted as needed throughout the course of the experiment. Nitrogen gas was used as the carrier gas for the reaction and a compressed N_2 tank fed N_2 gas through a gas flowmeter in order to control the carrier gas flow rate. As trials progressed, it was determined that the minimum flow rate achievable by this flowmeter (approximately 0.3-0.4 L/min minimum) was higher than what was needed in the trials. A rotameter was then added to the setup in order to allow for lower N_2 gas flow rates (approximately 10 mL/min minimum) in the trials.

Methanol was the only reactant fed to the reactor in this setup. Originally, methanol was fed to the reactor using a water bath to heat the methanol and send the vapors through the reactor. This method of feeding methanol to the reactor was quickly dropped in favor of using a syringe pump to feed liquid methanol. This switch allowed the amount of methanol fed to the reactor to be more easily and accurately controlled.

The methanol and the N_2 carrier gas met at a “tee” before being fed to the reactor. Early on, a 1-inch diameter tube was used for the reactor. This was packed with catalyst surrounding a temperature probe. The methanol contacted the catalyst inside the tubing and was kept at the temperature inside a furnace. A temperature probe was used to monitor and control this temperature. A switch was made to a smaller 0.25-inch diameter tube in order to potentially see better results. The smaller tube meant the temperature probe had to rest outside the tubing. This may have been less accurate as a result.

In the original setup with the larger tubing, the catalyst was packed in the reactor as full uncrushed, pelletized particles with a 2 mm diameter and 2-10 mm of length. When the switch was made to the smaller tubing, the catalyst was crushed to smaller sizes between 177 and 850 μm, allowing particle size to be varied from trial to trial. In all trials with the smaller tubing, catalyst mass charged in the reactor was kept constant at 2.00 grams.

Pelletized ZSM-5 catalyst with a SiO_2/Al_2O_3 ratio of 38 was crushed using a mortar and pestle, then sieved to the appropriate size using trays from the Rose-Hulman Chemical Engineering Laboratories. After 2.00 grams of the appropriate catalyst was sieved and weighed, it was funneled into the reactor tubing and held in place with quartz wool on either side of the catalyst. With smaller reactor tubing, packing the catalyst was difficult. Best results were found when the catalyst was slowly funneled into the tubing after quartz wool had been placed on one side. Quartz wool on either side was placed by curling it into a cylindrical shape and twisting it into the tubing.

After the gases left the reactor, they were fed into a flask that was submerged in an ice bath in order to condense the remaining methanol as well as any liquid products. This liquid was then analyzed using the GC/MS in the Rose-Hulman Chemistry Department. A Shimadzu GC-2010 Gas Chromatograph connected to a Shimadzu GCMS-QP2010S Gas Chromatograph Mass Spectrometer was used. The column was an Elite-5MS PerkinElmer column with a 1,4-bis(dimethylsiloxy)phenylene dimethyl polysiloxane phase. The GC/MS temperature method that was used started at a temperature of 55 $°C$, then was held for 5 minutes. It then ramped to 260 $°C$ at a rate of 15 $\frac{°C}{minute}$, and then was held at 260 $°C$ for 6 minutes, as seen in Figure 3-1.

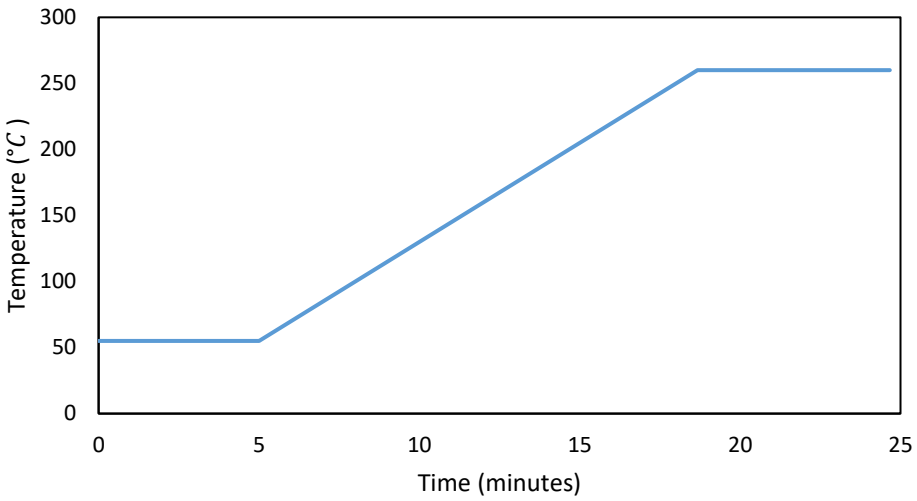

Figure 3-1. Temperature control method used for data analysis on the GC/MS.

Any non-condensed gases that were still carried by the N_2 carrier gas, were vented to the hood above the reactor and unfortunately unable to be analyzed with the available resources. Future students could analyze these gases by condensing them with dry ice or by direct analysis of the gases with an analytical system integrated directly into the setup.

During reaction trials, 99% assay methanol was always pumped at 0.05 $\frac{mL}{minute}$ for 100 minutes at the beginning of each trial. After this, the flask was changed out so that the sample collected at the end for analysis would contain liquid that was collected entirely while the reaction was at steady state. Testing determined that 100 minutes was more than sufficient time for the reaction to reach steady state. A full schematic and picture of the setup is shown in Figures 3-2 and 3-3.

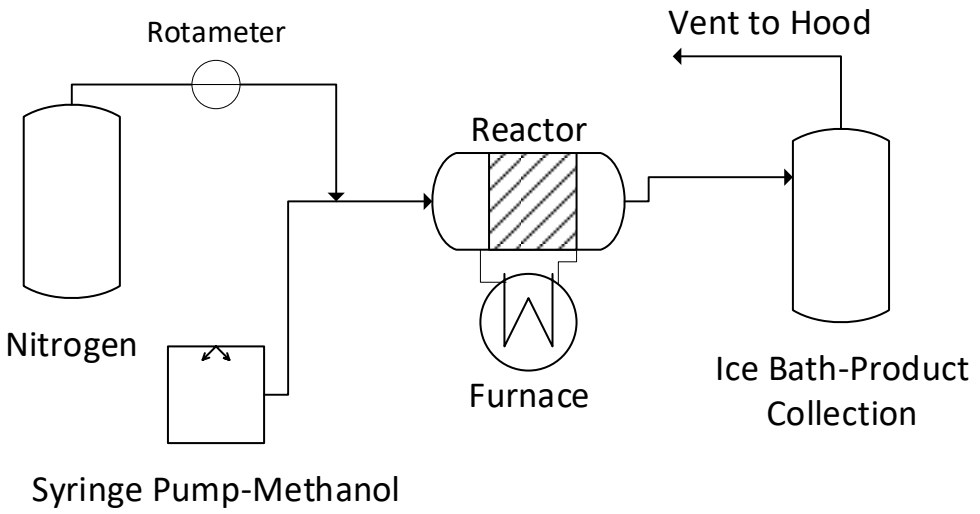

Figure 3-2. General schematic of the final process setup.

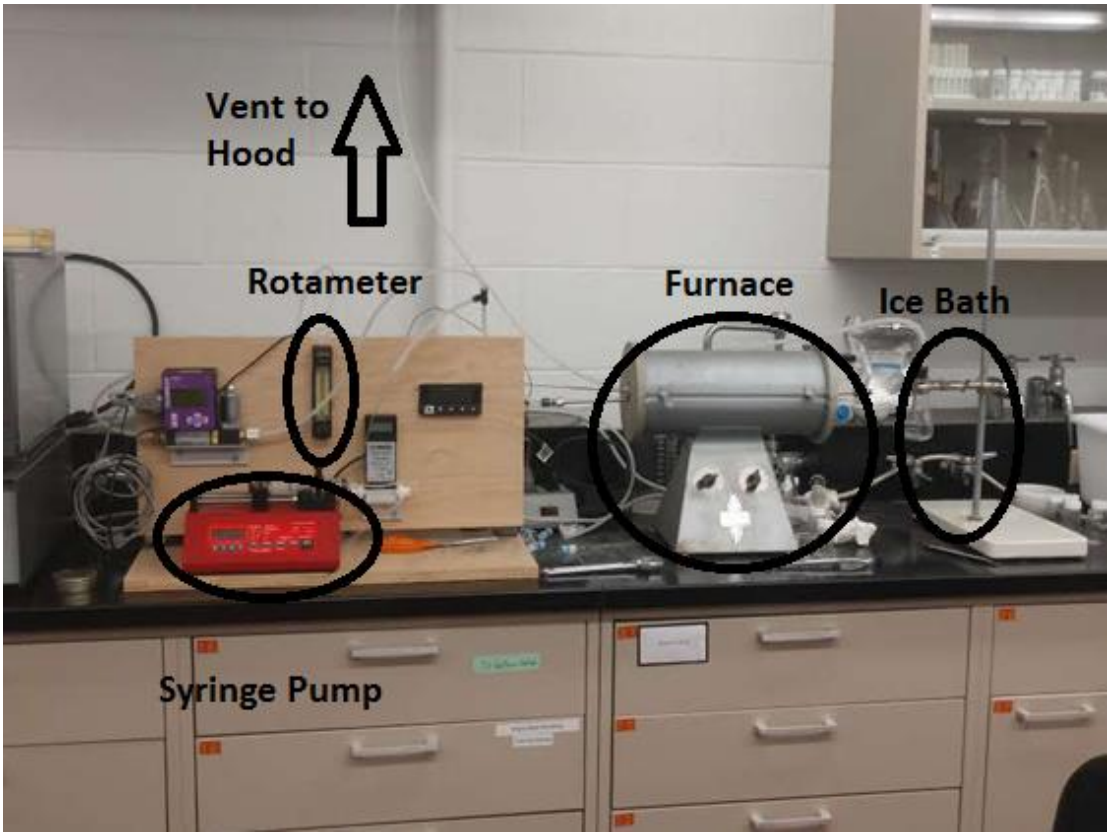

Figure 3-3. Picture of final process setup.

4. Results and Discussion

4.1. Calibration Curves

The results from the GC/MS were used for analysis. In order to make a more meaningful analysis of the peak area values from the GC/MS results, calibration curves for a range of the expected aromatics including both xylenes and polymethylbenzenes up to hexamethylbenzene were created. The calibration curves were developed in a concentration range that encompassed results from early on in the trials. This trial was run at 370 $°C$, 0.5 L/min N_2 flow rate, and 0.5 mL/min liquid methanol flow rate. The reactor was charged with 30 grams of catalyst. The peak areas from this trial served as a basis for the calibration curves and the elution times are shown below in Table 4-1. The peaks were identified using the mass spectra data base by matching m/z ratios of tabulated compounds in the software. For the all identified peaks, the identification software had a minimum value of 90 leading to reasonably conclusive results.

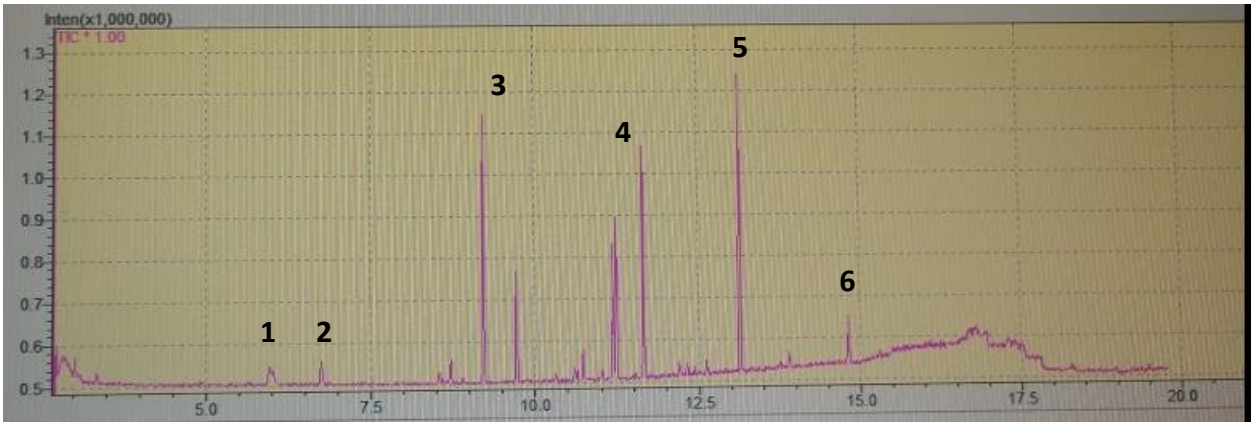

Figure 4-1. Example chromatogram for data analysis.

The peak areas from this trial served as a basis for the calibration curves and the elution times are shown below in Table 4-1 using the peak identities in Figure 4-1.

Table 4-1. Typical compound elution times.

Peak #	Compound	Peak Elution Time (min)
1	o-xylene	6
2	p-xylene	7
3	C_9 aromatics	8.5-9.5
4	C_{10} aromatics	11-12
5	C_{11} aromatics	13
6	C_{12} aromatics	15

For the $C_9 - C_{12}$ aromatics, the exact compounds were unable to be determined, so the decision was made to add the areas from the peaks of the same molecular weight species. The $C_9, C_{10}, C_{11},$ and C_{12} aromatics calibration curves were made with the respective polymethylbenzenes. A representative calibration curve is shown below in Figure 4-2 and the rest of the curves can be found in the Appendix.

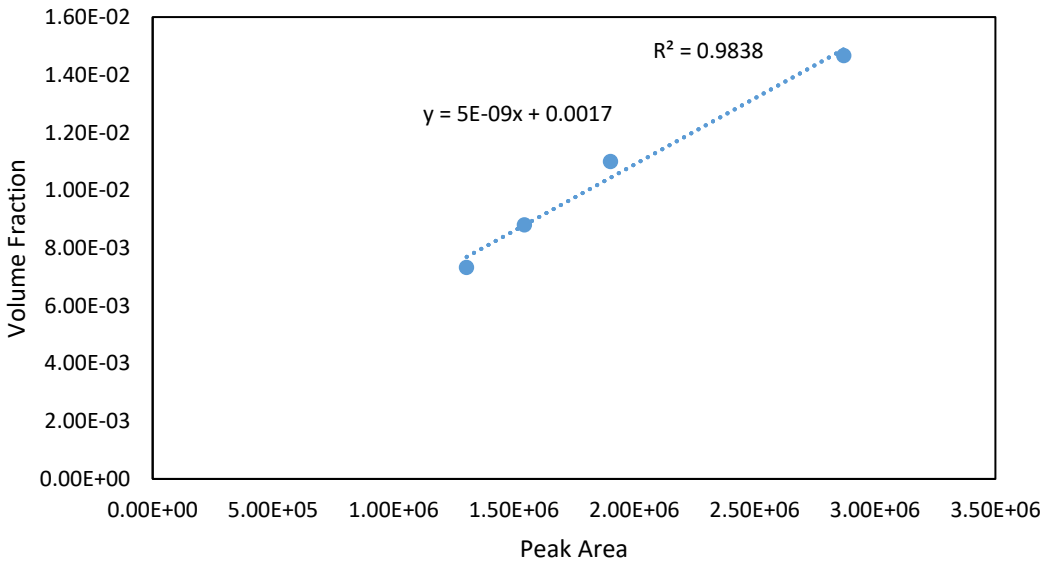

Figure 4-2. Calibration curve for o-xylene.

Using the first setup with the 1” diameter reactor trials were run at various nitrogen flow rates with other conditions being constant: 370 $°C$, 0.5 mL/min methanol flow rate, and uncrushed, full-size catalyst pellets. After multiple trials at 0.5 L/min and one at 1.5 L/min nitrogen flow rate, it was quickly apparent that the reaction setup that was being used led to very inconsistent results and changes were made in order to get more reproducible results. As seen in Figure 4-3, three trials that were run at the same conditions varied by as much as a factor of ten.

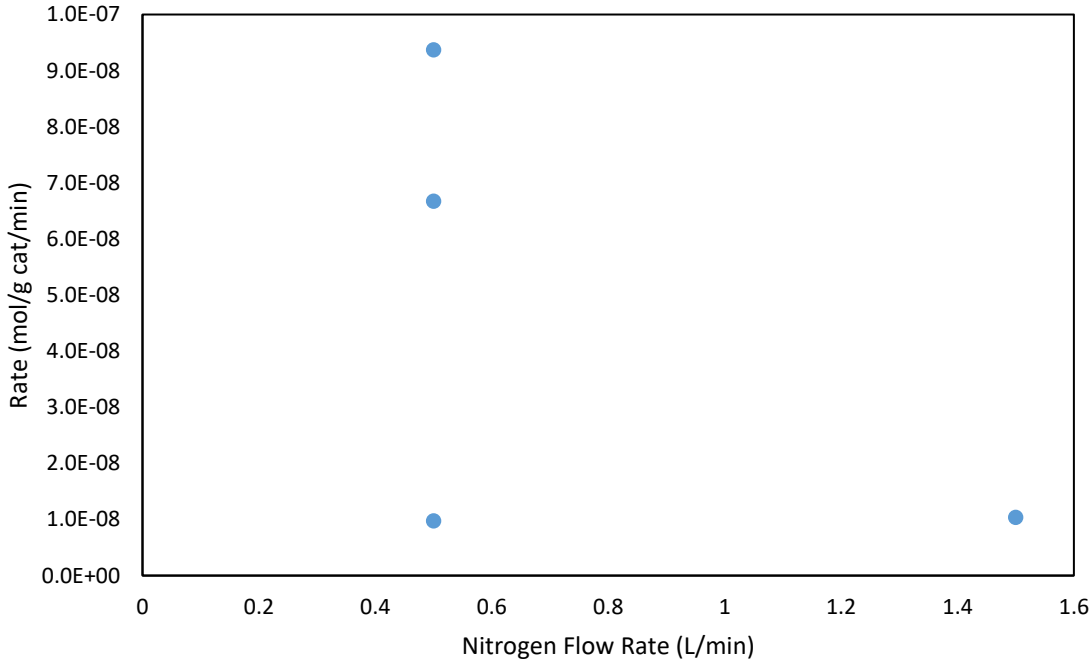

Figure 4-3. Rate values for larger reactor setup.

The trial at 1.5 L/min nitrogen flow rate did not show any significant difference. These results led us to believe the large size of our catalyst pellets might have left too much void space in the bed, causing significant amounts of methanol feed to not contact the catalyst as it passed through the reactor. Many previous reported works [17] showed promising results with this

reaction using a smaller reactor tube and crushed catalyst; they also had lower nitrogen and methanol flow rates. These findings caused us to change the reactor setup to the smaller diameter reactor tubing.

The smaller reactor tubing meant that lower flow rates were required for similar reaction conditions to be met. Unfortunately, the flow meter that was being used could only regulate nitrogen flow rates as low as about 40 mL/min. In order to produce lower flow rates, a rotameter was installed, which allowed for nitrogen flow rates as low as about 10 mL/min. Particle trays were also used to sieve crushed catalyst particles to desired particle diameter ranges for use in the trials. Three particle size diameter ranges were chosen to vary particle size for the trials to study the effect of particle size. The chosen particle size was based on the literature source [17], where a particle size of 150-300 μm was used. Our particle size range was chosen as 177-297 μm as these are the closest sieve sizes that could be quickly obtained from the Rose-Hulman Chemical Engineering Laboratory. Ideally, we would test particle size ranges on either side of the range above; however, if a particle size smaller than this range was chosen, pressure in the system became too high for the setup used. The setup was not able to handle high backpressure, and it led to tubing popping off or leakage through various joints.

The reason for the increase in the pressure becomes apparent when looking at equation 9 from Section 2, the Ergun equation. The two terms in the equation have d_p, particle diameter, in the denominator and one of those terms is particle diameter squared. This means that as the particle diameter in a fixed bed decreases, the pressure drop per unit length increases significantly. In order to run tests with smaller catalyst size, the setup would have to be modified to better handle larger amounts of backpressure.

Now that a reaction setup was found with more consistent results, a plan for trials was made to test the effect of temperature, carrier gas flow rate, and particle diameter. Due to time constraints using these reaction conditions, allowed for only three different values to be tested. The reaction conditions tested can be seen below in Table 4-2 with relevant values for condition comparisons in bold:

Table 4-2. Reaction conditions used for trials. Conditions that were relevant for comparisons from each trial are bolded.

Temperature$(^{\circ}\boldsymbol{C})$	**Particle Size Range** $(\boldsymbol{\mu m})$	**Nitrogen Flow Rate** $\left(\frac{\boldsymbol{mL}}{\boldsymbol{min}}\right)$
375	**177-297**	**25**
350	177-297	25
400	177-297	25
375	177-297	**10**
375	177-297	**50**
375	**297-600**	10
375	**600-850**	10

Results from these trials had values that fell outside the range of the previously made calibration curves, so the previously made curves were unable to be used for the quantitative analysis of these results**.** Additional calibration curves were unable to be created due to time constraints and GC/MS availability. Therefore, these trials were analyzed qualitatively by looking at the summed numerical peak areas of the various aromatics that were expected as products.

4.2. Temperature

The first set of three trials varied temperature while keeping particle size and nitrogen flow rate constant at 177-297 μm and 25 $\frac{mL}{minute}$, respectively. Temperature values were chosen to center around the 375 $°C$ range because various literature sources determined that to be optimal for this reaction. The other temperatures were chosen to test temperatures on either side of the optimal. Results from these trials are presented in Figure 4-4. The vertical axis corresponds to the peak areas of the major compounds ($C_8 - C_{10}$).

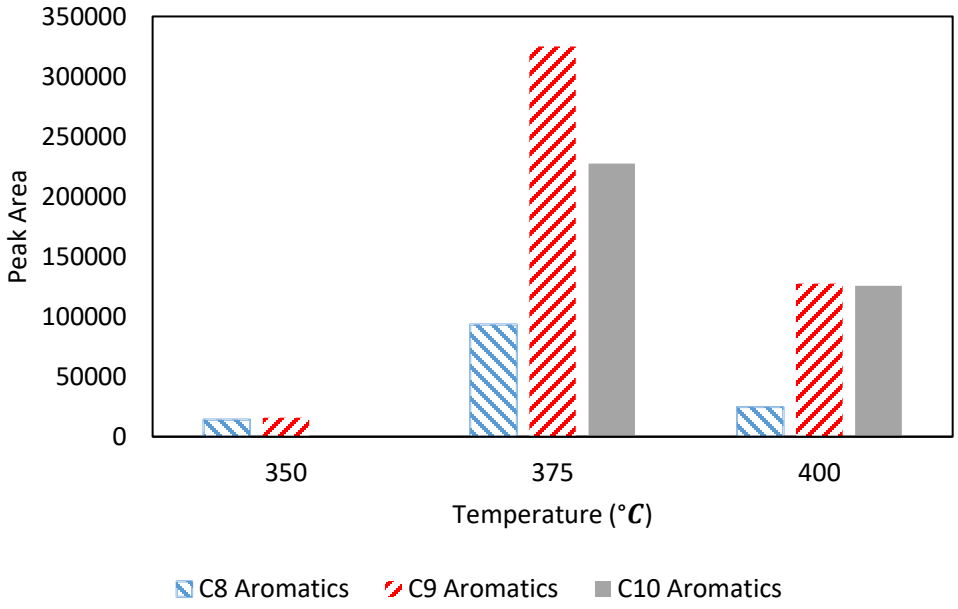

Figure 4-4. Summed peak areas for aromatics vs. temperature.

A clear trend can be seen which is the same for each of the $C_8 - C_{10}$ aromatics peak areas. All three groups of aromatics show low values for the 350 $°C$ trial, higher values for the 375 $°C$ trial, and values that are somewhere in the middle for the 400 $°C$ trial. This is the type of trend

that would be expected based on literature sources that have found 375 $°C$ to be an optimal temperature condition for the reaction. Since the previous calibration curves cannot be used in this range, nothing definitive can be said, quantitatively, with regards to selectivity. But the data does show a trend that matches what would be expected and also helps to explain why 375 $°C$ shows the higher conversion to these aromatics. If the areas for the 350 $°C$ and the 400 $°C$ trials are compared for each of the different sized aromatics; at higher temperatures, selectivity towards higher molecular weight aromatics appears to increase. At 350 $°C$ there was no peak found for C_{10} aromatics, showing that at this temperature the reaction has trouble progressing that far. At 400 $°C$, there appears to be relatively more C_{10} aromatics than lower molecular weight aromatics. This is likely due to the reaction progressing faster at a higher temperature as is seen and expected in most chemical reactions. In this specific reaction, the reaction progressing faster means that more of the higher molecular weight aromatics are formed up to even the $C_{11} - C_{12}$ aromatics. These aromatics are unable to pass diffuse through the catalyst channels and cause catalyst deactivation. This is likely why 375 $°C$ seems to have the highest methanol conversion to aromatic products for this reaction. These trends can be seen in Figure 4-5 where peak area fraction is plotted at different temperatures in order to show what the selectivity trend looks like. Peak area fraction is not the same as selectivity but for the purposes of qualitative analysis is enough for comparison in this case.

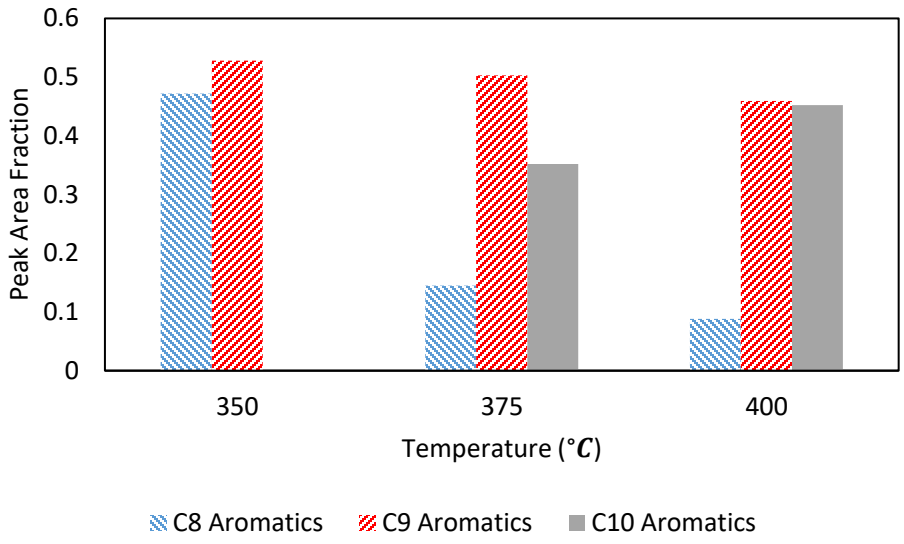

Figure 4-5. Peak area fractions for aromatics vs. temperature.

4.3. Nitrogen Flow Rate

The next two trials paired with the first trial were used to examine the effects of nitrogen gas flow rate. These trials used nitrogen flow rates of 10, 25, and 50 mL/min. The temperature and particle size for these trials were kept constant at 375 °C and 177-297 μm, respectively. Figure 4-6 displays the results from these trials. Once again, a clear trend can be observed for nitrogen flow rate and the peak areas of all of the aromatics. As the flow rate increases, there is a clear decrease in conversion of methanol to $C_8 - C_{10}$ aromatics. This trend is expected if all of the nitrogen flow rates are in the regime where the reaction rate is reaction limited instead of diffusion limited. The expected trend for reaction rate with respect to carrier gas flow rate is that starting at very low flow rates the reaction rate increases until it levels out.

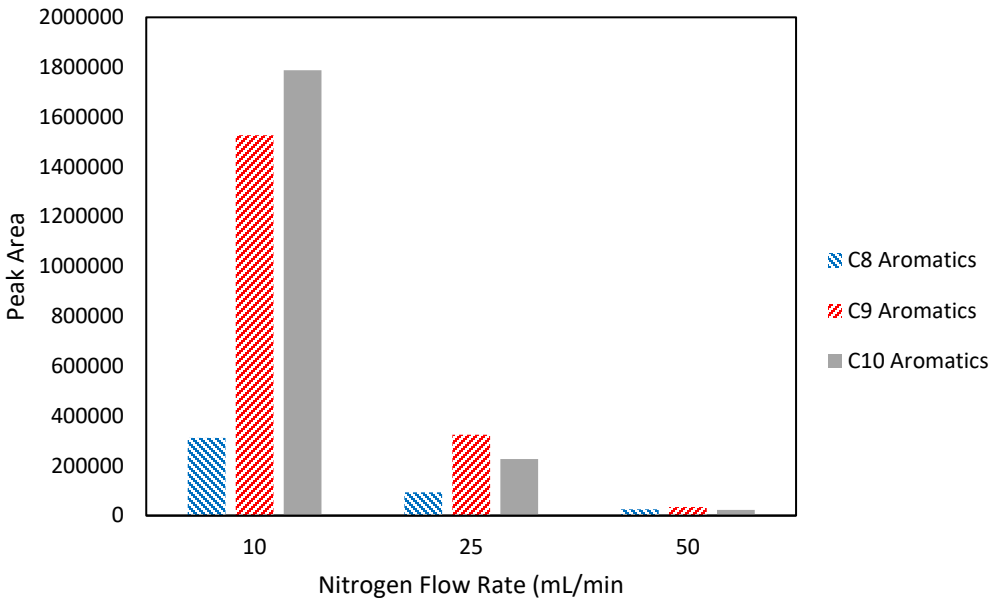

Figure 4-6. Aromatics summed peak areas vs. nitrogen flow rate.

The point where reaction rate levels out is the point between the two regimes. The area at low flow rates is the diffusion limited regime, while the area after it levels out is the reaction limited regime. The diffusion limited regime occurs when the flow rate is slow enough that reaction happens faster than the external diffusion of the reactant into the catalyst. Therefore, the reaction entering the catalyst is the step that limits the reaction rate. The example graph from earlier illustrating this effect was shown in Figure 2-1. At these flow rates, the gas flow rate is fast enough that the rate exists in the reaction limited regime. As the flow rate increases the residence time decreases and the conversion goes down even though the rate stays the same.

In Figure 4-7, selectivity based on peak area fraction towards each of the aromatics is shown. Upon careful inspection of this figure, it is clear that higher nitrogen flow rates increase selectivity towards the lower molecular weight aromatics and lower flow rates increase selectivity towards the higher molecular weight aromatics. This is expected because at lower flow

rates the residence time is higher allowing more time for the reaction to progress towards the larger compounds.

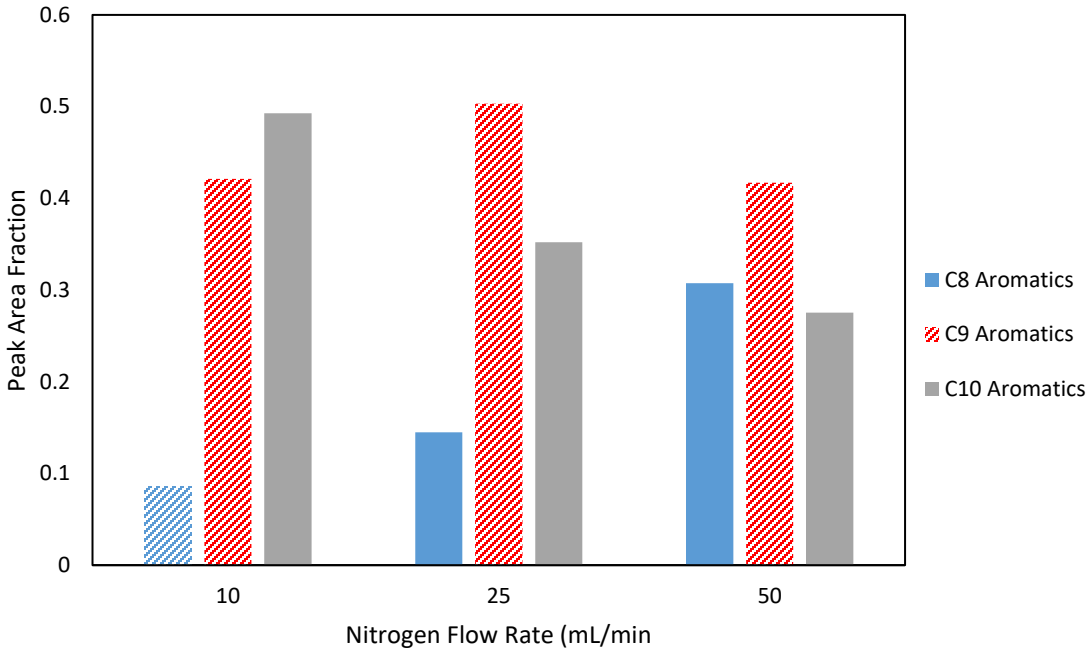

Figure 4-7. Peak area fractions for aromatics vs. nitrogen flow rate.

4.4. Particle Size

The final reaction condition tested was particle size. Particle size was varied with ranges of 177-297 μm, 297-600 μm, and 600-850 μm. Temperature and nitrogen flow rate were kept constant at 375 $^{\circ}C$ and 10 mL/min. The nitrogen flow rate was chosen as 10 mL/min instead of 25 mL/min because the last set of trials showed that 10 mL/min produced the highest conversion. The results from these trials are shown in Figure 4-8. The x-value for particle size on the graph is represented by the average of the upper and lower bounds of the particle size ranges.

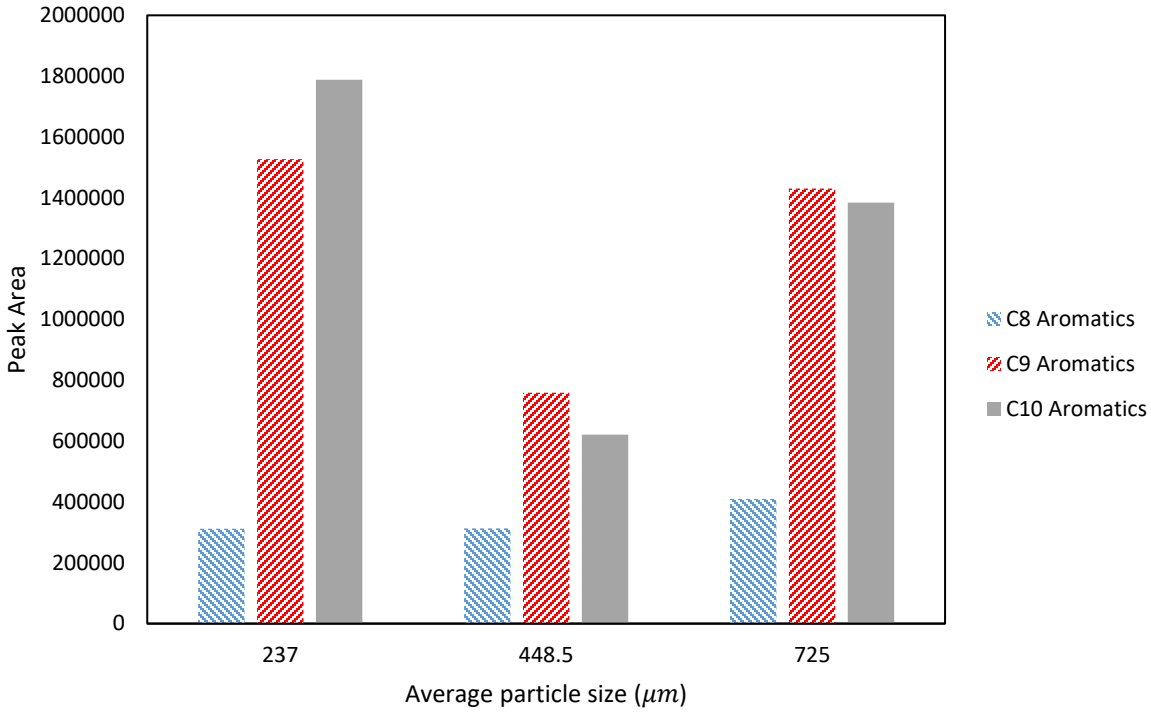

Figure 4-8. Aromatics summed peak areas vs. particle size.

The results from the particle size trials yielded no explainable trends for the conversion of methanol to aromatics. Trends for selectivity might be apparent if lower molecular weight products were also able to be analyzed. Using an ice bath to condense products means that some products are not as easily obtained such as the light gases. As mentioned earlier, these products could be analyzed by instead condensing with dry ice or direct analysis of the gases with an attached analytical method to the setup. This meant the only products able to be examined with any degree of certainty for this setup were the aromatics. More information might be able to be obtained with respect to the effects of particle size if the gaseous products were able to be sent directly to analytical equipment. Additionally, the location of the temperature probe next to the

reactor tubing instead of inside it may have had a negative effect on the consistency of the results, leading to possible trends getting lost.

The carbon pool mechanism relies on organic impurities in order to start the formation of the "hydrocarbon pool." The methanol used for the reaction had a purity of greater than 99.9% assay. Conversions that were obtained were significantly lower than those of various literature sources, so an additional trial was run with 1% by volume ethanol added to our methanol feed as an impurity to make sure that lack of impurities was not affecting the early progression of the reaction. This trial was run at the following conditions: 10 mL/min nitrogen flow rate, 375 $°C$, and 177-297 μm particle diameter. The summed peak areas under these conditions did not have a noticeable trend. Peak area of the C_8 aromatics increased by approximately 50%, peak area of the C_9 aromatics decreased by approximately 10%, and peak area of the C_{10} aromatics decreased by approximately 58%. While the peak areas for each aromatic did change from the previous trial of the same conditions, the overall conversion of methanol to aromatics stayed consistent. This means that the lower conversions of our trials compared to literature trials was not due to a lack of impurities to start the "hydrocarbon pool". A plot of this data compared to the trial without ethanol is shown in Figure 4-9.

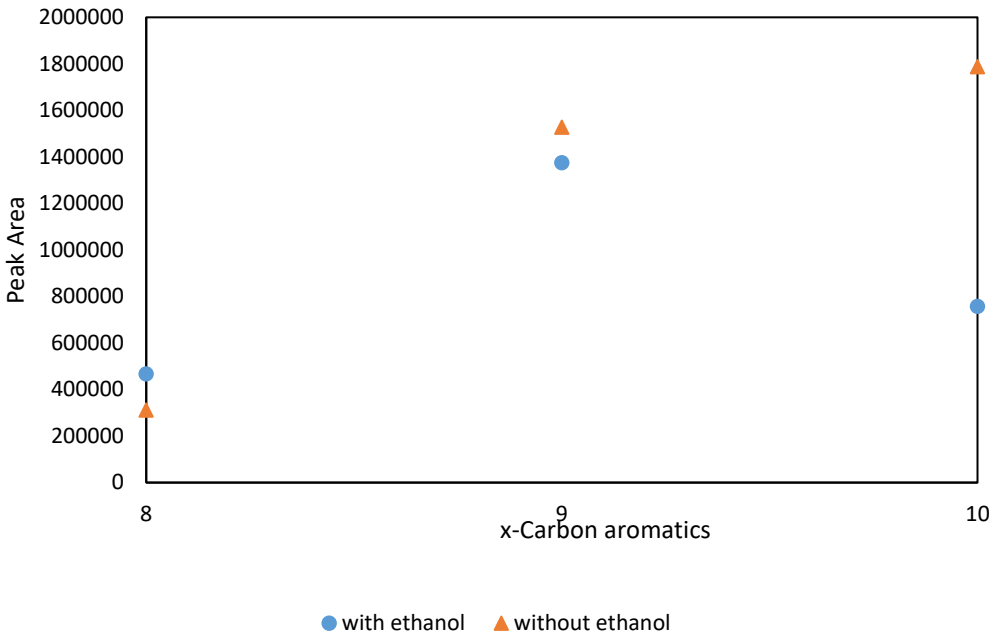

Figure 4-9. Comparison of ethanol trial to trial without ethanol addition.

As demonstrated by the previous analysis, a simple setup of a fixed bed reactor like the one examined here can allow for analysis of many different factors that provides analysis on chemical engineering principles that can prove valuable in an undergraduate learning experience. Varying temperature and looking at conversion and selectivity provides insight into the kinetics of the reaction. Varying nitrogen flow rate can be used to show concepts related to the various regimes that effect reaction rate. The trials that were ran in this paper were located in the reaction rate limited regime, but setup modifications could allow for the diffusion-limited regime and the transition point between regimes to be shown as well. Different equipment that could lower the nitrogen flow rate further could allow for analysis in the diffusion-limited regime. The varying of particle size did not show any trends here; but if setup changes were made, it might prove valuable in showing the effects of the Thiele modulus. In addition to these effects, other

studies can be done to provide information on the reusability of the catalyst after the used catalyst has been regenerated. This could be done by comparing the conversion and selectivity found with a fresh catalyst to those of catalyst that has been regenerated. These studies could also be repeated with the addition of metals to the catalyst like zinc or copper to see the effects on conversion, selectivity, and catalyst deactivation.

5. Educational Use

By examining data and finding trends like those analyzed in the previous section, this experiment can be used to teach some core principles related to heterogeneous catalyzed reactions in a Unit Operations Laboratory setting. This type of experiment can provide a steppingstone into learning about industries that use catalysts to create various chemicals, especially the petroleum industry. Some different learning objectives, as well as the relevant variables and outcomes of those objectives, can be seen in Table 5-1.

Table 5-1. Learning objectives for possible projects with this reaction setup.

Learning Objective	Control Variable	Outcomes
Internal Diffusion	Particle Size	Thiele modulus
External Diffusion	Flow Rate	Diffusion/reaction rate limited regimes
Kinetics	Temperature	Selectivity, conversion, yield
Reusability	All	Activity vs. time

Variation of particle size can be used to teach students about internal diffusion through the catalyst and how that affects the reaction rate. As previously discussed, the Thiele modulus scales with particle size and is used to show how as particles get bigger, internal diffusion through the catalyst becomes more difficult and decreases the reaction rate. In Equation 18 from Section 2 it can be seen that as particle size increases Thiele Modulus increases. This equation can be developed using chemical engineering principles and then becomes useful as a learning tool.

Varying flow rate and plotting results can be used to examine the effects of external diffusion on the reaction rate. At low flow rates, the reaction over the catalyst is limited by external diffusion due to the rate that reactants can enter the catalyst sites. As flow rate increases, rate increases until it's no longer limited by diffusion into the catalyst and instead is limited by reaction rate. This point represents the separation of the two regimes and can be clearly seen in experiments where the flow rate is varied. This core concept is represented in Equation 11 from Section 2 where the mass transfer coefficient is inversely proportional to the boundary layer thickness. From core principles learned in fluids classes it is known that as fluid velocity increases, the boundary layer decreases and diffusion into the catalyst is no longer limiting.

The kinetics of catalytic reaction can be examined by varying the temperature of reaction trials. This allows for students to investigate outcomes such as selectivity, conversion, and yield for the reactions. In the context of this reaction, it was able to be seen where the optimal temperature was with respect to conversion. The core concepts of kinetics are represented in Equation 8 from Section 2, where the rate is shown in relation to temperature among other variables. Also, within Equation 8 is the effects of pressure on the reaction. As was shown with the Ergun equation in Equation 9. These two equations show that a large pressure drop across the reactor, as was seen in this study, decreases the reaction rate.

A possible learning objective that was not analyzed in this research is catalyst reusability. This can be tested alongside any of the other learning objectives by rerunning experiments with regenerated catalyst and examining catalyst activity and if the rate stays the same with continued uses. This is extremely relevant for how it would work on an industrial scale in which it isn't

feasible to use fresh catalyst whenever it is used up. Instead, it is much more practical to use a regenerated catalyst and is therefore important to understand how or if regenerating it has any effects.

6. Conclusion

Unit operations in chemical engineering laboratories are used in many universities to teach many core chemical engineering principles. Some core principles that might be taught in unit operations labs include fluid mechanics, thermodynamics, and heat and mass transfer. In addition to experiments that teach these core principles, it is also useful to have experiments that might be considered more specialized. Specialized experiments still use fundamental principles from chemical engineering courses, but they also sometimes use concepts that are not seen as often or at all in a general chemical engineering curriculum. An experiment like the MTG reaction in a fixed bed reactor would provide a useful educational framework for teaching the concepts behind heterogeneous catalyzed reactions.

A variety of setup configurations were tested in the earlier trials of this reaction. Inconsistent results on the early trials led to the switch from a 1-inch diameter reactor to a 0.25-inch reactor, as well as the switch to crushed catalyst instead of pelletized catalyst. The smaller reactor led to the use of a rotameter for nitrogen flow rate control instead of the original flowmeter due to the lower minimum flow rate (10 mL/min vs. 0.5 L/min). A temperature probe and a controller were used to control the temperature of the reactor. A syringe pump was used to feed the liquid methanol into the reactor, and an ice bath was used to condense products in a vial at the reactor outlet before being vented to the hood. This experimental setup brought the best combination of consistency and methanol conversion but was not without its own problems.

There are a few improvements that should be made for this setup but were unable to be attempted due to factors such as time or cost. A smaller temperature probe that could either fit

into the reactor or be implemented immediately at the exit of the reactor instead of next to the tubing would likely yield more consistent results across the board due to more accurate temperature control. The analysis would benefit from analytical equipment tied directly into the setup such that all products could be analyzed in real time. This would give information on how the reaction progresses over and give information on the product slate that had too low of boiling points to condense from the ice bath. The furnace that was used for heating was designed for the bigger tubing, so a furnace that better matched the size of the reactor tubing would likely give more consistency to the temperature control. Finally, a flowmeter or rotameter that went to lower flow rates could be beneficial if reactor size was kept similar. The best results obtained were at the lowest flow rates and, unfortunately, the readability of the rotameter in that low of a range was not very good either. Being able to run in a lower range would likely yield better and more accurate results due to larger conversion and better readability on flow rate.

Qualitative analysis showed some of the expected trends from the reaction conditions that were varied: temperature, nitrogen gas flow rate, and particle diameter. Various literature sources from trials with this reaction showed that the best conversion values to be at temperatures of about 370-375 $°C$. This was confirmed in the temperature trials in which the highest peak values were obtained for the $C_8 - C_{10}$ aromatics at 375 $°C$. The higher temperature also showed selectivity to the higher molecular weight aromatics. This means the reaction likely progressed faster at the higher temperature, which led to quicker catalyst deactivation. Varying the nitrogen flow rate showed the same trend for all of the aromatics. The highest methanol conversion occurred at the lowest flow rate. This means that higher flow rates lowered the residence time and with it the methanol conversion even though the rate stayed the same as it

occurred in the reaction rate limited regime. No trends were noticed when particle the size was varied.

7. References

[1] *BP Energy Outlook 2017 Edition*. 2017, www.bp.com/content/dam/bp/pdf/energy-economics/energy-outlook-2017/bp-energy-outlook-2017.pdf.

[2] "Methanol to Gasoline Synthesis | ExxonMobil Chemical." *Where We Operate | ExxonMobil Chemical* , 8 Nov. 2017, www.exxonmobilchemical.com/en/products-and-services/technology-licensing-and-services/methanol-to-gasoline-synthesis.

[3] "Ftsynthesis." *What Are the Primary Sources of CO2?*, 20 June 2013, www.netl.doe.gov/research/coal/energy-systems/gasification/gasifipedia/ftsynthesis.

[4] "Refining Crude Oil." *Refining Crude Oil - Energy Explained, Your Guide To Understanding Energy - Energy Information Administration*, www.eia.gov/energyexplained/index.php?page=oil_refining.

[5] Olah, George A. "Beyond Oil and Gas: The Methanol Economy." *Angewandte Chemie International Edition*, John Wiley & Sons, Ltd, 31 Mar. 2005, onlinelibrary.wiley.com/doi/abs/10.1002/anie.200462121.

[6] "Gasoline - Energy Explained, Your Guide To Understanding Energy - Energy Information Administration." *EIA*, www.eia.gov/energyexplained/index.php?page=gasoline_home.

[7] IAGS, and Institute for the Analysis of Global Security. "Sources of Methanol." *IAGS*, www.iags.org/methanolsources.htm.

[8] "Syngas Conversion to Methanol." *National Energy Technology Laboratory*, www.netl.doe.gov/research/coal/energy-systems/gasification/gasifipedia/methanol.

[9] Ali, Khozema Ahmed. “Recent Development in Catalytic Technologies for Methanol Synthesis from Renewable Sources: A Critical Review.” *Renewable and Sustainable Energy Reviews*, Science Direct, 22 Jan. 2015, www.sciencedirect.com/science/article/pii/S1364032115000209.

[10] “Hydrogen Storage.” *Energy.gov*, www.energy.gov/eere/fuelcells/hydrogen-storage.

[11] “Alternative Fuels and Advanced Vehicles.” *Alternative Fuels Data Center: Fuel Prices*, www.afdc.energy.gov/fuels/.

[12] Wang, Peter. “Catalysts in 21st Century Energy.” *Stanford*, large.stanford.edu/courses/2016/ph240/wang2/.

[13] Hakan Olcay, Ayyagari V. Subrahmanyam, Rong Xing, Jason Lajoie, James A. Dumesic and George W. Huber (2013) Production of renewable petroleum refinery diesel and jet fuel feedstocks from hemicellulose sugar streams. *Energy Environ. Sci.* 6, 205-216 doi: 10.1039/C2EE23316A

[14] Libretexts. “The Effect of a Catalyst on Rate of Reaction.” *Chemistry LibreTexts*, National Science Foundation, 2 June 2017, chem.libretexts.org/Textbook_Maps/Inorganic_Chemistry/Supplemental_Modules_(Inorganic_Chemistry)/Catalysis/The_Effect_of_a_Catalyst_on_Rate_of_Reaction

[15] Lindström, Bård, and Lars J. Pettersson. “A Brief History of Catalysis.” *SpringerLink*, Kluwer Academic Publishers-Plenum Publishers, link.springer.com/article/10.1023/A:1025001809516.

[16] “Types of Catalysis.” *Types of Catalysis*, Chemguide, www.chemguide.co.uk/physical/catalysis/introduction.html.

[17] Andrigo, P. “Fixed Bed Reactors.” *ScienceDirect*, Catalysis Today, 1999, doi.org/10.1016/S0920-5861(99)00076-0.

[18] Chang, Clarence. “Process Studies on the Conversion of Methanol to Gasoline.” *ACS Publications*, July 1978, pubs.acs.org/doi/abs/10.1021/i260067a008

[19] *MFI: Type Material*, asia.iza-structure.org/IZA-SC/material_tm.php?STC=MFI.

[20] Chu, Cynthia T-W. “Isomorphous Substitution in Zeolite Frameworks. 1. Acidity of Surface Hydroxyls in [B]-, [Fe]-, [Ga]-, and [Al]-ZSM-5.” *ACS Publications*, 6 Dec. 1984, pubs.acs.org/doi/10.1021/j100255a005.

[21] Olson, D. H., et al. “Crystal Structure and Structure-Related Properties of ZSM-5.” *ACS Publications*, Journal of Physical Chemistry, 1981, pubs.acs.org/doi/pdf/10.1021/j150615a020.

[22] Song, Weiguo, et al. “An Oft-Studied Reaction That May Never Have Been: Direct Catalytic Conversion of Methanol or Dimethyl Ether to Hydrocarbons on the Solid Acids HZSM-5 or HSAPO-34.” *ACS Publications*, 26 June 2001, pubs.acs.org/doi/pdf/10.1021/ja016499u.

[23] Schulz, Hanz. “‘Coking’ of Zeolites during Methanol Conversion: Basic Reactions of the MTO-, MTP- and MTG Processes.” *ScienceDirect*, Academic Press, 15 Sept. 2010, www.sciencedirect.com/science/article/pii/S0920586110003305.

[24] Fogler, H. Scott. *Elements of Chemical Reaction Engineering*. Pearson Education Internat., 2006.

8. Appendix

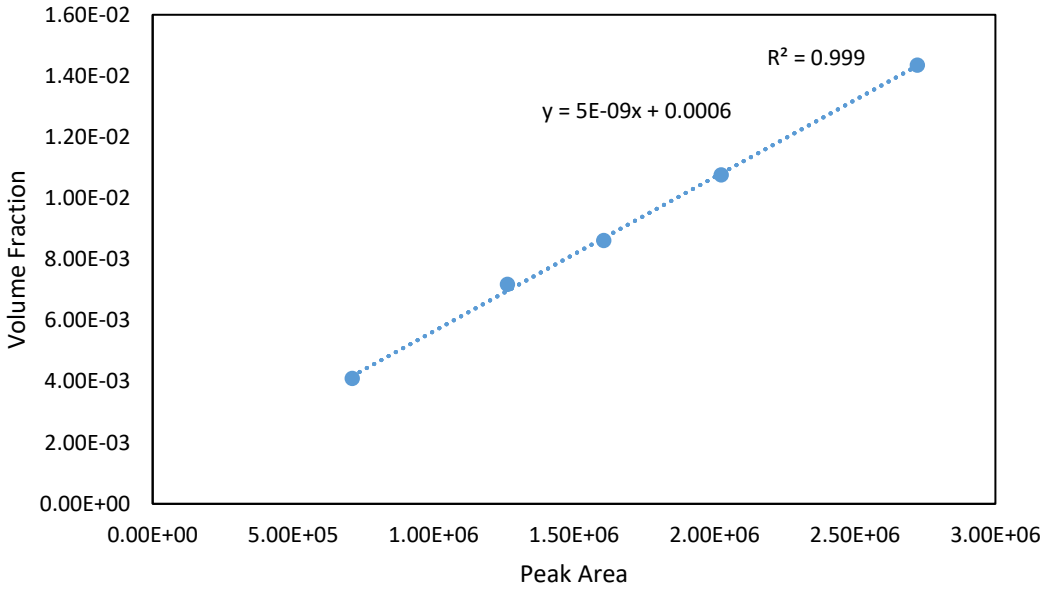

Figure 8-1. Calibration curve for p-xylene.

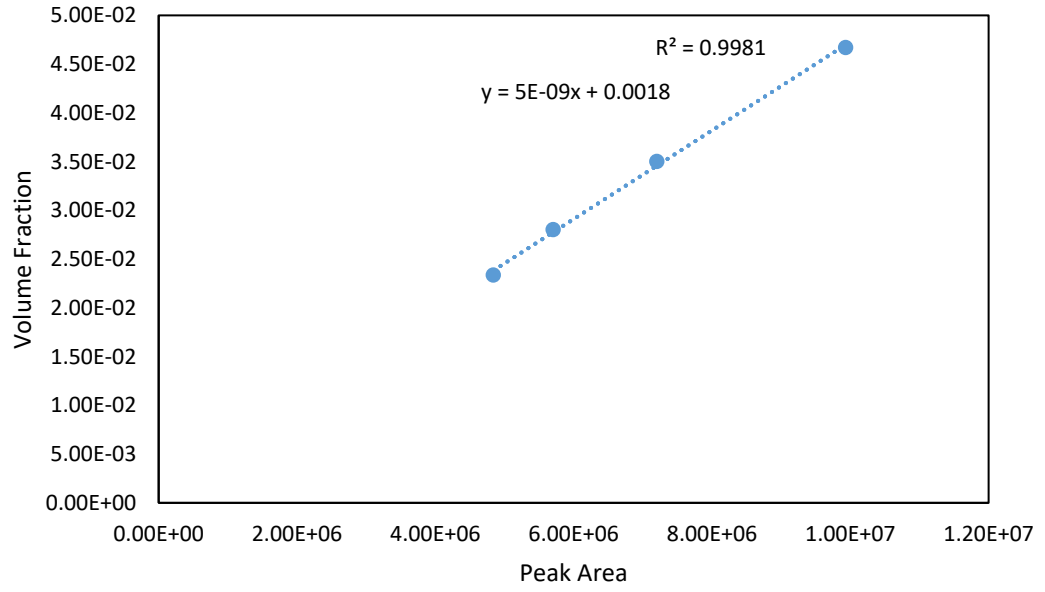

Figure 8-2. Calibration curve for C_9 aromatics.

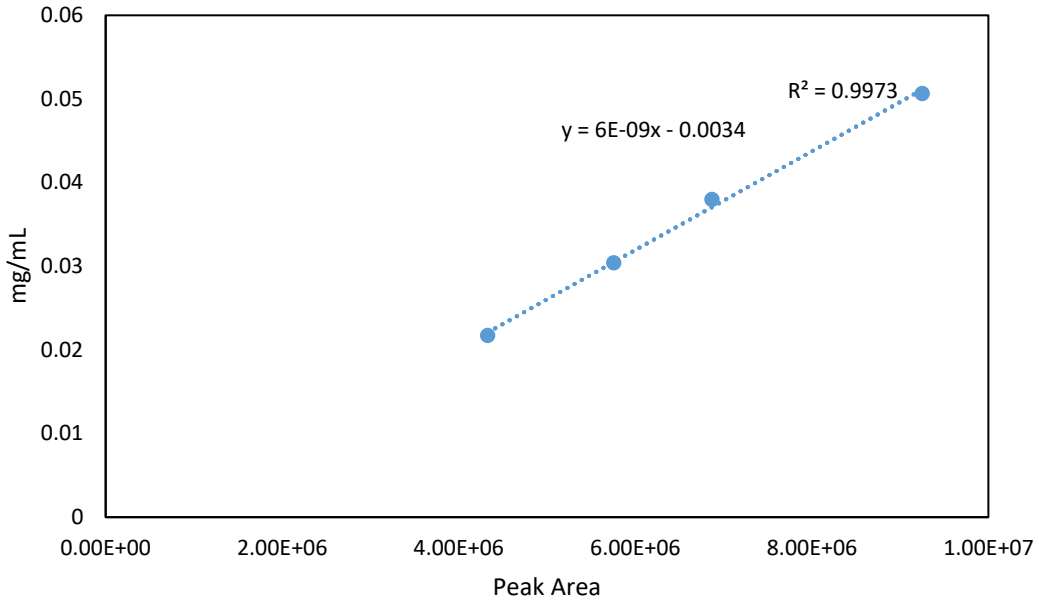

Figure 8-3. Calibration curve for C_{10} aromatics.

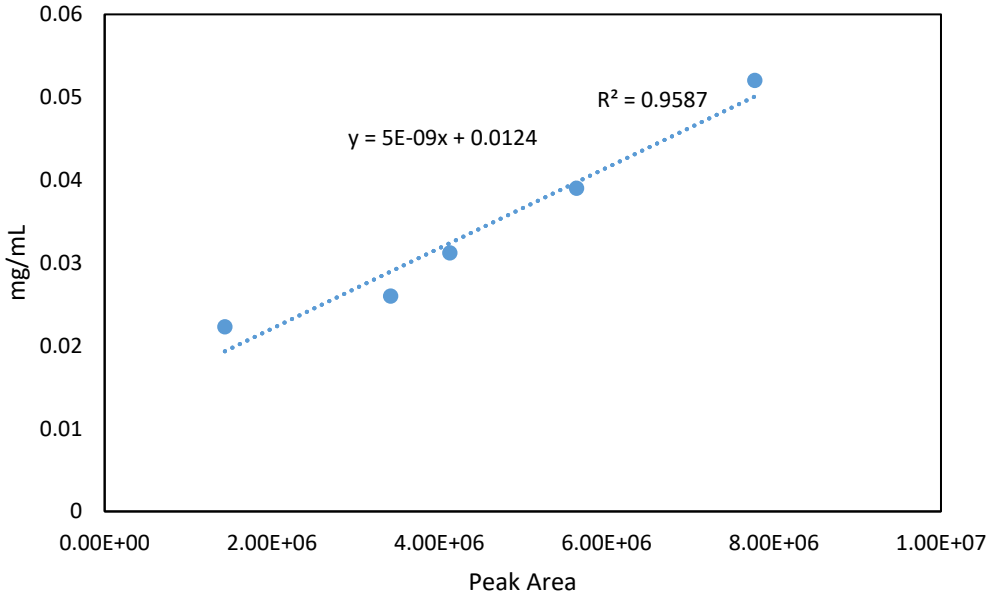

Figure 8-4. Calibration curve for C_{11} aromatics.

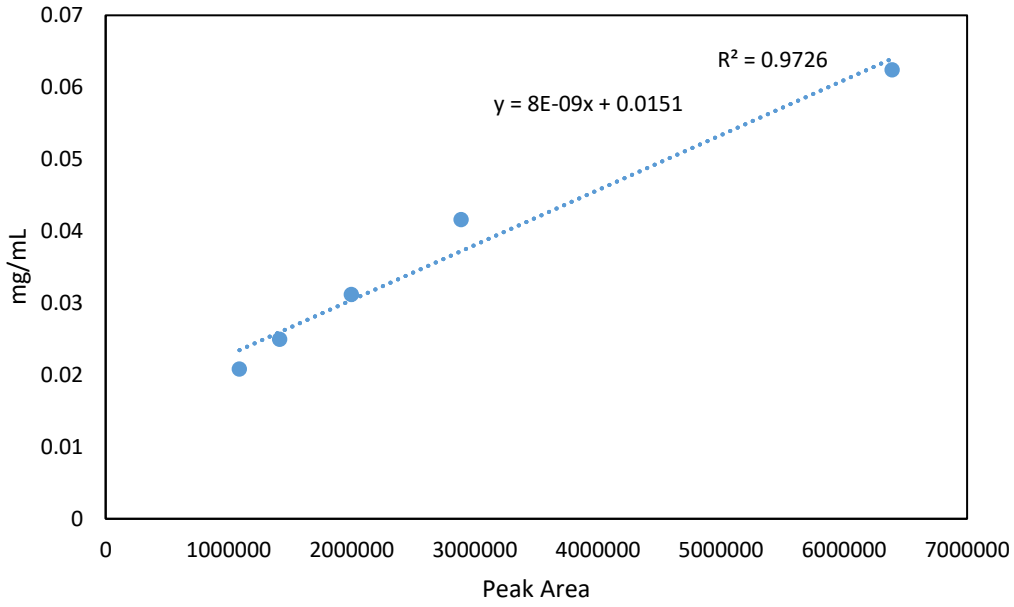

Figure 8-5. Calibration curve for C_{12} aromatics.